NMR Conformational Study of the Cytoplasmic Domain of the Canine Sec61γ Protein from the Protein Translocation Pore of the Endoplasmic Reticulum Membrane

Veronica Beswick,[‡] Françoise Baleux,[§] Tam Huynh-Dinh,[§] François Képès,[||] Jean-Michel Neumann,*[,‡] and Alain Sanson*[,‡,⊥]

Département de Biologie Cellulaire et Moléculaire, Section de Biophysique des Protéines et des Membranes, URA CNRS 2096, and Service de Biochimie et de Génétique Moléculaire, CEA Saclay, 91191 Gif sur Yvette Cedex, France, and Unité de Chimie Organique, URA CNRS 487, Institut Pasteur, 28 rue du Dr Roux, 75724 Paris Cedex 15, France

Received July 12, 1996; Revised Manuscript Received September 24, 1996[⊗]

ABSTRACT: Conformational studies of the synthesized N-terminal cytoplasmic domain of the canine Sec61γ protein, an essential protein from the translocation pore of secretory proteins across the endoplasmic reticulum membrane, were performed using two-dimensional proton NMR spectroscopy. This canine domain is one of the smallest domains within the homologous protein family and may thus constitute the minimal functional structure. The peptide was solubilized in pure aqueous solution or in the presence of dodecylphosphocholine micelles mimicking a membrane−solution interface. In pure aqueous solution, the peptide is remarkably unfolded. Forming a stable complex with dodecylphosphocholine micelles, it acquires a well-defined α-helix−loop−α-helix secondary structure, with the first helix, highly amphipathic, lying at the micelle surface. The loop comprising four residues is delimited by two flanking helix-capping structures, highly conserved in the whole homologous protein family. No tertiary structure, which could have been revealed by interhelix NOE contacts, was observed. From these experimental results and using general arguments based on sequence information and knowledge of peptide−membrane interactions, a structure of the entire Sec61γ protein in membrane bilayers is proposed.

The earliest event in the export of secretory proteins from eukaryotic cells is their transport across the endoplasmic reticulum (ER)[1] membrane, followed by signal peptide cleavage, core glycosylation, and folding. It has been shown that, in yeast cells, the translocation of secretory proteins involves a protein-conducting channel, the Sec61 complex (Esnault *et al.*, 1994; Panzner *et al.*, 1995). This complex is called the translocation pore and is also involved in the insertion of proteins into membrane. The translocation pore is formed by the association of three membrane proteins: (i) Sec61p (Deshaies & Schekman, 1987; Stirling *et al.*, 1992), a 53 kDa protein with 10 transmembrane domains (Stirling *et al.*, 1992); (ii) Sss1p (Esnault *et al.*, 1993), an 8.9 kDa protein anchored to the ER membrane by its C-terminal hydrophobic domain with its N terminus on the cytoplasmic side (Esnault *et al.*, 1994); and (iii) Sbh1p (Panzner *et al.*, 1995), a 10 kDa protein with the same topology as Sss1p.

In mammalian cells, a homologous Sec61 complex was found (Görlich & Rapoport, 1993; Hartmann *et al.*, 1994) that also comprises three membrane proteins: Sec61α (Sec61p homologue), Sec61γ (Sss1p homologue), and Sec61β (to which Sbh1p was found to be homologous). Interestingly, it has been shown that Sec61γ can functionally replace Sss1p in yeast cells (Hartmann *et al.*, 1994).

At the present level of our knowledge on the translocation machinery, one can now focus on the molecular mechanisms involved, that is investigate the structure−function relationship of the proteins forming the translocation pore. Sss1p/Sec61γ proteins appear as good first candidates for such an investigation since their low molecular mass allows a conformational study at the residue level by NMR spectroscopy and because their role is essential for pore function; severe defects in translocation of several secretory and membrane protein insertions result from Sss1p depletion (Esnault *et al.*, 1993).

Sss1p and Sec61γ proteins were predicted to possess a single transmembrane C-terminal segment, most probably α-helical, whereas their N-terminal cytoplasmic domain appears strongly amphipathic with a large number of basic amino acids and is thus expected to present strong interactions with the phospholipidic interface. In the present work, we focused on the N-terminal cytoplasmic domain of the canine Sec61γ protein obtained by chemical synthesis. The choice of Sec61γ results from a double observation: (i) As already mentioned, yeast Sss1p and canine Sec61γ cross-complement; (ii) the canine Sec61γ sequence is significantly shorter than that of yeast Sss1p (67 and 79 residues, respectively), and the difference exclusively concerns the N-terminal domain. Therefore, the cytoplasmic domain of canine Sec61γ is believed to represent the minimum

* Author to whom correspondence should be addressed. Fax: 33 1 69 08 81 39. Phone: 33 1 69 08 28 63.
[‡] URA CNRS 2096, CEA Saclay.
[§] URA CNRS 487, Institut Pasteur.
[||] CEA Saclay.
[⊥] Also from Université P. et M. Curie, 9 Quai Saint-Bernard, Bât. C, 75005 Paris, France.
[⊗] Abstract published in *Advance ACS Abstracts,* November 1, 1996.
[1] Abbreviations: COSY, correlated spectroscopy; CPMG, Carr−Purcell−Meiboom−Gill pulse sequence; DPC, d_{38}-dodecylphosphocholine; DSS, 2,2-dimethyl-2-silapentane-5-sulfonate; EDTA, ethylenediaminetetraacetic acid; ER, endoplasmic reticulum; JR, "jump and return" pulse sequence; NMR, nuclear magnetic resonance; NOE, nuclear Overhauser effect; NOESY, nuclear Overhauser enhancement spectroscopy; POPC, 1-palmitoyl-2-oleoyl-*sn*-glycero-3-phosphocholine; R_1, longitudinal relaxation rate; R_2, transverse relaxation rate; SA, simulated annealing; TFA, trifluoroacetic acid; TOCSY, total correlated spectroscopy.

S0006-2960(96)01710-2 CCC: $12.00

functional unit for this component of the translocation pore. Our aim is thus to analyze the conformational properties and the stability of the N-terminal cytoplasmic Sec61γ domain either in pure aqueous solution or in a membrane-like environment.

The canine Sec61γ sequence is $DQVMQ_5FVEPS_{10}$-$RQFVK_{15}DSIRL_{20}VKRCT_{25}KPDRK_{30}EFQKI_{35}AMATA_{40}$-$IGFAI_{45}MGFIG_{50}FFVKL_{55}IHIPI_{60}NNIIV_{65}GG$.

The cytoplasmic domain can be predicted to span the D_1−K_{34} segment, and the transmembrane domain to span the I_{35}−H_{57} segment. The present paper reports the results of our NMR conformational study of the synthesized canine Sec61γ N-terminal cytoplasmic domain, extended to residue G_{42}, solubilized either in pure aqueous solution or in the presence of dodecylphosphocholine micelles mimicking a membrane−solution interface. From the experimental results and using general arguments based on sequence−structure relationship information and knowledge of peptide−membrane interactions, a model for the structure of the entire Sec61γ protein in the membrane bilayer is proposed.

MATERIALS AND METHODS

Peptide Synthesis. In order to minimize possible boundary effects, the predicted sequence of the Sec61γ N-terminal cytoplasmic domain (35 residues) was extended to 42 residues with the sequence $D_1QVMQ_5FVEPS_{10}RQFVK_{15}$-$DSIRL_{20}VKRST_{25}KPDRK_{30}EFQKI_{35}AMATA_{40}IG$.

To prevent a potentially disturbing dimerization, Cys24 was replaced by a Ser residue. The identically modified Sss1p was found to perfectly complement a yeast strain deprived of any *SSS1* wild-type gene (F. Skiba and F. Képès, unpublished data). The Cys24Ser mutation is therefore not expected to change the function of the protein.

The peptide was synthesized by the Merrifield solid-phase method (Merrifield, 1963) on an Applied Biosystems 430A synthesizer. The synthesis was performed using 0.5 mmol of Boc Gly Pam resin. Stepwise elongation of the peptide chain was done using the standard coupling−capping protocols. The ^{15}N Val in position 21 was incorporated using a file normally assigned to this amino acid and filling the amino acid cartridge with its Boc derivative (EurisoTop, France). Half of the peptide resin (1.1 g) was subjected to the low−high HF cleavage (Tam & Heath, 1983). The crude peptide (484 mg) was purified on BIO Gel P4 using 0.1 M AcOH as eluent. The peptide (150 mg) was then purified on a Nucleosil 5 μm C18 300 Å semipreparative column, using a 15 to 50% linear gradient of acetonitrile in 0.08% aqueous TFA for 20 min at a 6 mL/min flow rate. The final purity of the peptide (99%) was checked on a Nucleosil 5 μm C18 300 Å analytical column, using a 20 to 55% linear gradient of the same eluents as above, at a 1 mL/min flow rate ($\mathbf{t}_R$ = 14.24 min). The yield was 45 mg. The positive ion electrospray ionization mass spectrum was 4879.8 Da (expected, 4879.6 Da).

NMR Experiments. Samples were prepared from 7 mg of pure peptide dissolved in D_2O or in 90:10 H_2O/D_2O 10 mM phosphate buffer containing 0.1 mM EDTA to give a final concentration of 3 mM. A second set of samples was prepared by cosolubilizing 7 mg of pure peptide and 24 or 48 mg of deuterated d_{38}-dodecylphosphocholine (DPC) (SMM, CEA, France) in the same buffer as described above. The pH was adjusted to 5.0 in most experiments. Sets of COSY, TOCSY, and NOESY phase sensitive spectra were collected either on a Bruker AMX 500 or on a Bruker AMX 600 spectrometer at different temperatures from −1 to 24 °C (pure aqueous solution) and from 22 to 45 °C (in the presence of micelles). Chemical shifts were referenced from the DSS signal. The water resonance was suppressed either by presaturation or by using the JR sequence (Plateau & Guéron, 1982). In general, a total of 48 (COSY and TOCSY) or 80 (NOESY) transients were acquired with a recycling delay of 1 s. Increments (512) of 2K data points were collected for each two-dimensional experiment, yielding a digital resolution of 6 or 8 Hz/point in both dimensions after zero filling. Shifted squared sine-bell functions were used for apodization. The mixing times were 80 and 150 ms for the TOCSY and NOESY experiments, respectively.

The longitudinal and transverse ^{15}N relaxation rates (R_1, and R_2) of the ^{15}N-labeled Val 21 residue were measured on a Bruker AMX 500 spectrometer in the absence and presence of DPC micelles at 25 °C using one-dimensional ^{1}H−^{15}N experiments derived from the two-dimensional pulse schemes proposed by Kay *et al.* (1989). A recycling delay of 4 s and a refocusing delay of 1 ms (CPMG) were used. Longitudinal and transverse ^{31}P relaxation rates (R_1 and R_2) of DPC micelles were measured at 202 MHz on a Bruker AMX 500 spectrometer in the absence and presence of peptide at 25 °C. Standard inversion recovery and CPMG sequences were used with a recycling delay of 10 s and a refocusing delay of 2 ms (CPMG). No ^{1}H−^{31}P NOE was detected, thus confirming that the ^{31}P relaxation is solely governed by the chemical shift anisotropy at 202 MHz.

Molecular Modeling. We used the last release, 6.1, of Sybyl (Tripos) for analyzing the NOE data in terms of secondary structure and for modeling the entire Sec61γ protein. Tripos force field with electrostatics was used for minimization and dynamics. The entire protein was constructed, and the secondary structure, partly resulting from the experimental study of the cytoplasmic domain, was set. Hydrogen bonds, according to secondary structures, were added whenever possible. After construction, initial structures with the desired topology (see text) were obtained by setting interhelix constraints. After a rough minimization, the loop residues, R23−D28, were subjected to simulated annealing from 700 to 0 K for 3 ps. The initial structures, with interhelix constraints, were then minimized by alternating short low-temperature (2 ps, 50 K) dynamics and minimization runs on the entire structure until the potential energy remains stable. Then, the interhelix constraints were removed, and the whole structures, with only secondary structure constraints, were subjected to a 300 K dynamics for 20 ps, to check the stability of the structure and eventually to make sure that the structure corresponded to, at least, a local energy minimum. Surviving structures were further minimized.

RESULTS AND DISCUSSION

NMR Data of the Peptide Solubilized in Pure Aqueous Solution. The N-terminal cytoplasmic domain of canine Sec61γ protein was found easily soluble in aqueous solution at the NMR concentrations. Proton resonance assignment was performed on a 3 mM sample using standard COSY, TOCSY, and NOESY experiments recorded at different temperatures (−1, 9, 11, 20, and 24 °C). Proton chemical

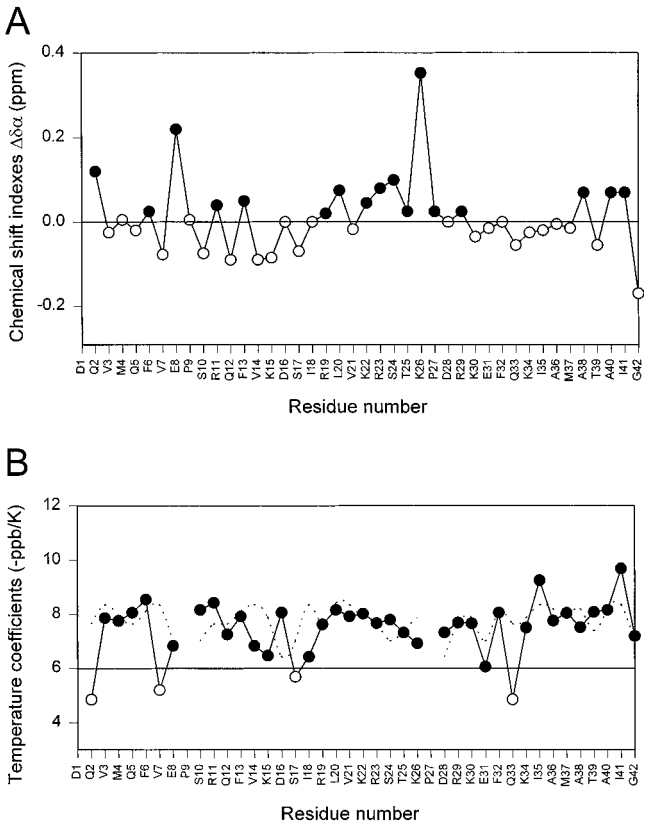

FIGURE 1: (A) α-Proton chemical shift indexes, $\Delta\delta\alpha = \delta\alpha_{obs} - \delta\alpha_{coil}$, for the peptide solubilized in aqueous solution at −1 °C and pH 5. Filled and hollow symbols respectively correspond to positive and negative $\Delta\delta\alpha$ values. (B) Temperature coefficients of the amide protons for the peptide solubilized in aqueous solution (solid line) and for random coil peptides (dashed line) (Merutka *et al.*, 1995). Filled and hollow symbols respectively correspond to temperature coefficients smaller and larger than −6 ppb/K.

shifts of the peptide measured at −1 °C are given as Supporting Information. The weak spectral dispersion of the amide proton signals (0.7 ppm) and the scarce NOE pattern apart from intense αN(i,i+1) correlations indicate that the peptide is poorly structured in aqueous solution. Nevertheless, a few NN(i,i+1) correlations and one medium range αN(14,17) correlation, both characterizing α-helix structures, were found. The overall conformational tendency of the peptide was described using the Hα chemical shift index ($\Delta\delta\alpha$). For each residue, this index was determined by subtracting the random coil chemical shift value, $\delta\alpha_{coil}$ (Merutka *et al.*, 1995), from that measured at −1 °C, $\delta\alpha_{obs}$ ($\Delta\delta\alpha = \delta\alpha_{obs} - \delta\alpha_{coil}$). Figure 1A shows the $\Delta\delta\alpha$ index profile of the 42-residue peptide. The weak $\Delta\delta\alpha$ values confirm the absence of any stable secondary structure for the peptide solubilized in pure aqueous solution. However, in the S10−S17 segment, the $\Delta\delta\alpha$ values are predominantly negative, suggesting a weak preference of the peptide for the helix secondary structure, in agreement with the observed αN(14,17) NOE. Nevertheless, the largest negative $\Delta\delta\alpha$ values do not exceed −0.1 ppm and are thus quite far from the values observed for a stable helix (about −0.4 ppm, Wishart *et al.*, 1992). Lastly, most of the measured $^3J_{\alpha N}$ values are between 6 and 8 Hz which indicates the absence of any stable structure in agreement with the NOE and $\Delta\delta\alpha$ data.

With regard to the V7 residue, an apparent contradictory result was noticed, that is a $^3J_{\alpha N}$ value of 9 Hz (β-region) associated with a $\Delta\delta\alpha$ value of −0.1 ppm (α-region). In fact, the negative $\Delta\delta\alpha$ value has to be related to a ring current effect induced by the neighboring F6 residue since the V7 Hβ and H$\gamma\gamma'$ proton chemical shifts (1.925 and 0.91 ppm, respectively) also appear significantly high-field shifted from their standard values (Merutka *et al.*, 1995). Such an effect suggests the existence of a hydrophobic cluster involving F6 and V7. Furthermore, the presence of a strong NN(7,8) NOE and the set of NOEs observed between F6 and V7, V7 and E8, and F6 and E8 side chain protons also support this view. Existence of highly populated residual structures, based on hydrophobic side chain clustering, is now quite commonly observed in the unfolded state of proteins (Garvey *et al.*, 1989; Evans *et al.*, 1991; Broadhurst *et al.*, 1991; Neri *et al.*, 1992; Alexandrescu *et al.*, 1993; Macquaire *et al.*, 1993; Smith *et al.*, 1994; Lumb & Kim, 1994). These structures are thought to constitute important initiation sites of secondary structure in the early state of folding.

The temperature dependence of the amide proton chemical shifts was also studied, and Figure 1B shows the temperature coefficients obtained for each residue. The dashed line shows the values measured for amide protons in random coil peptides (Merutka *et al.*, 1995). Most of the coefficients are close to the coil values which confirms that the peptide is poorly structured in aqueous solution. However, four residues—Q2, V7, S17, and Q33—exhibit a temperature coefficient lower than −6 ppb/K, indicating a significantly slower exchange between their amide proton and the solvent. For both glutamine residues, Q2 and Q33, it probably results from an intraresidue side chain to backbone hydrogen bond. In the case of S17, the low temperature coefficient supports the existence of a partial helical structure in the region previously delimited by the $\Delta\delta\alpha$ index. Lastly, the low temperature coefficient of V7 is in agreement with the presence of a (F6-V7-E8) cluster.

NMR Study of the Peptide in the Presence of Dodecylphosphocholine Micelles: Evidence for the Formation of a Stable Peptide−DPC Micelle Complex. In a first experiment, perdeuterated DPC (150 mM) was added to the peptide sample. Taking into account the peptide concentration (3 mM) and the aggregation number of a DPC micelle (about 50, Lauterwein *et al.*, 1979), the [peptide]/[DPC] molar ratio approximately corresponds to one peptide molecule for one micelle. Addition of DPC micelles considerably modifies the peptide spectrum, especially the spectral dispersion of the NH signals that is increased from 0.7 to 1.3 ppm. Such a large increase indicates that the DPC molecules strongly interact with the peptide and undoubtedly largely modify its conformation.

In order to more precisely characterize the peptide−micelle association, relaxation rate measurements were performed. For this purpose, a ^{15}N-labeled valine residue was incorporated into the synthesized peptide at position 21, i.e. in the middle of the sequence. ^{15}N R_1 and R_2 relaxation rates were measured in the absence and presence of micelles at 25 °C. As shown in Table 1, addition of micelles led to a large increase the R_2 value. Using the well-known formalism of Lipari and Zsabo (1982) and neglecting the effect of internal motions, a crude evaluation of the correlation time τ_R, characterizing the overall motion of the peptide, was derived from the R_1 and R_2 values. We found τ_R values of 3 and 10 ns for the free peptide and the peptide−micelle complex,

Table 1: Longitudinal (R_1) and Transverse (R_2) Relaxation Rates of the Peptide ^{15}N V21 Residue and of the DPC ^{31}P Head Group Measured at 25 °C

	R_1 (s^{-1})	R_2 (s^{-1})
^{15}N V21 (peptide) in the absence of DPC	1.7	3.2
^{15}N V21 (peptide) in the presence of DPC	1.4	11.5
^{31}P (DPC) in the absence of peptide	0.9	3.2
^{31}P (DPC) in the presence of peptide	1.2	7.6

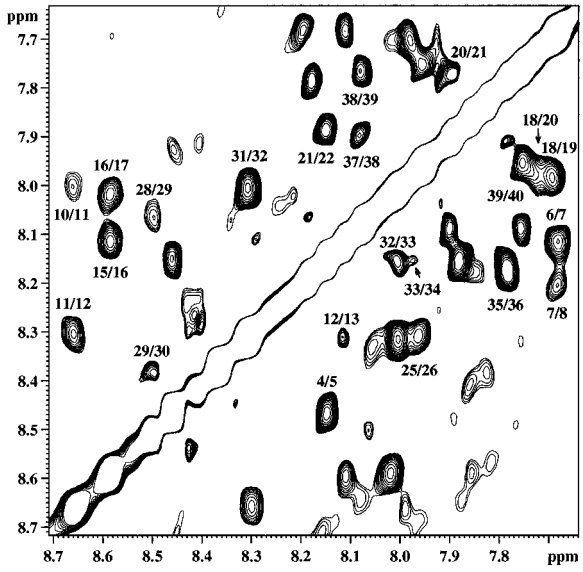

FIGURE 2: Amide proton region of the NOESY spectrum (500 MHz, mixing time and 150 ms) for the peptide solubilized in DPC micelles at 38 °C and pH 5.

respectively. In parallel, the ^{31}P R_1 and R_2 relaxation rates of the DPC head group were measured in the absence and presence of the peptide (Table 1) at 25 °C. Upon addition of peptide, the ^{31}P R_2 value is significantly increased, and in agreement with the ^{15}N relaxation study, the DPC relaxation parameters are consistent with the formation of a complex having a correlation time corresponding to a molecular mass of about 20−25 kDa, that is the expected range for one peptide solubilized in a micelle.

In a second set of experiments, the DPC concentration was doubled but no further spectral change was observed. This shows that the characteristic saturation plateau was already reached at the lower DPC concentration and that full solubilization of the peptide was achieved [see also for instance Cordier-Ochsenbein *et al.*, (1996)]. This also indicates that the occurrence of peptide oligomerization within the micelle is unlikely. In addition, such an oligomerization inside the micelle is known to give rise to characteristic NOE contacts clearly not detected here. The absence of oligomerization is also consistent with the markedly charged nature of the fragment which has four positive charges in excess.

Structure of the Peptide Solubilized in Dodecylphosphocholine Micelles. From standard COSY, TOCSY, and NOESY experiments recorded at 22, 30, 38, and 45 °C, almost all the proton resonances were assigned (Supporting Information). Figure 2 shows the amide proton region of the NOESY spectrum recorded at 38 °C. The structuring effect induced by the DPC micelles on the peptide, already indicated by the large increase of the NH spectral dispersion, was clearly confirmed by the abundant NOE network summarized in Figure 3. Two regions exhibit intense

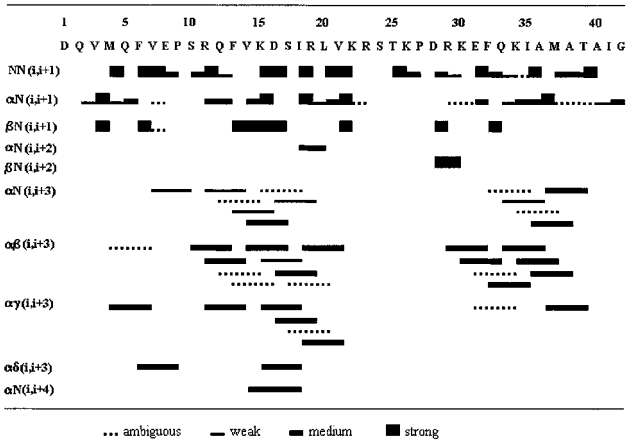

FIGURE 3: Diagram showing the sequential and medium range NOE connectivities for the peptide solubilized in the presence of DPC micelles at 38 °C and pH 5. The Pro δCH_2 protons are used as the NH proton.

sequential NN(i,i+1) NOEs and (i,i+3)/(i,i+4) correlations characteristic of α-helices: M4−K22 and R29−T39. Within the first helix, one can notice the presence of a Pro9 residue which could disrupt the integrity of the helix. However, significant Nδ(8,9) NOEs indicate a preferred trans conformation for the P9 residue and the P9 signals associated with the cis configuration are indeed very small, corresponding to only a few percents of this configuration. In addition, an αN(7,10) NOE is observed. We thus conclude that the M4−K22 segment forms a unique helix. Nevertheless, the significant increase of the number of (i,i+3) NOEs observed when passing from M4−P9 to S10−K22 indicates that the presence of the Pro residue increases the flexibility of the N-terminal end.

As for the NOE network, the ΔHα index (Figure 4A) clearly establishes the formation of stable helical secondary structures for the peptide in the presence of DPC. For the first helix region defined by the NOE data, M4−K22, the corresponding ΔHα profile exhibits (i,i+3) oscillations of negative amplitude (apart from the singular P9-S10 motif), characteristic of a stable amphipathic helix with a frayed N-terminal end. The ΔHα profile relative to the second helix defined by the NOE data, R29−T39, also displays characteristic (i,i+3) oscillations of negative ΔHα amplitudes that are however weaker than those observed for the first helix. The R23−D28 segment connecting both helices, designated A (M4−K22) and B (R29−T39) in the following, exhibits null or positive ΔHα values consistent with a loop structure.

Examination of the amino acid sequence of the cytoplasmic domain of the canine Sec61γ protein suggests the occurrence of several possible motifs able to form local structures, initiating or stabilizing the two α-helices. First, we observed that the B-helix starts with a characteristic D_{28}-XXE_{31} capping box motif known to form a very stabilizing N-terminal structure. The structure of N-terminal capping boxes such as the DXXE motif has been recently described for several helices (Harper & Rose, 1993; Lyu *et al.*, 1993; Jiménez *et al.*, 1994; Seale *et al.*, 1994; Muñoz & Serrano, 1995; Muñoz *et al.*, 1995) and consists of a i/i+3 reciprocal side chain to main chain hydrogen-bonding network. The occurrence of an N-capping structure is strongly supported by the intense βN(28,30) NOE (Figure 3), by the strong magnetic nonequivalence of the D28 $\beta\beta'$ signals (0.1 ppm), and especially by the very low temperature coefficients of

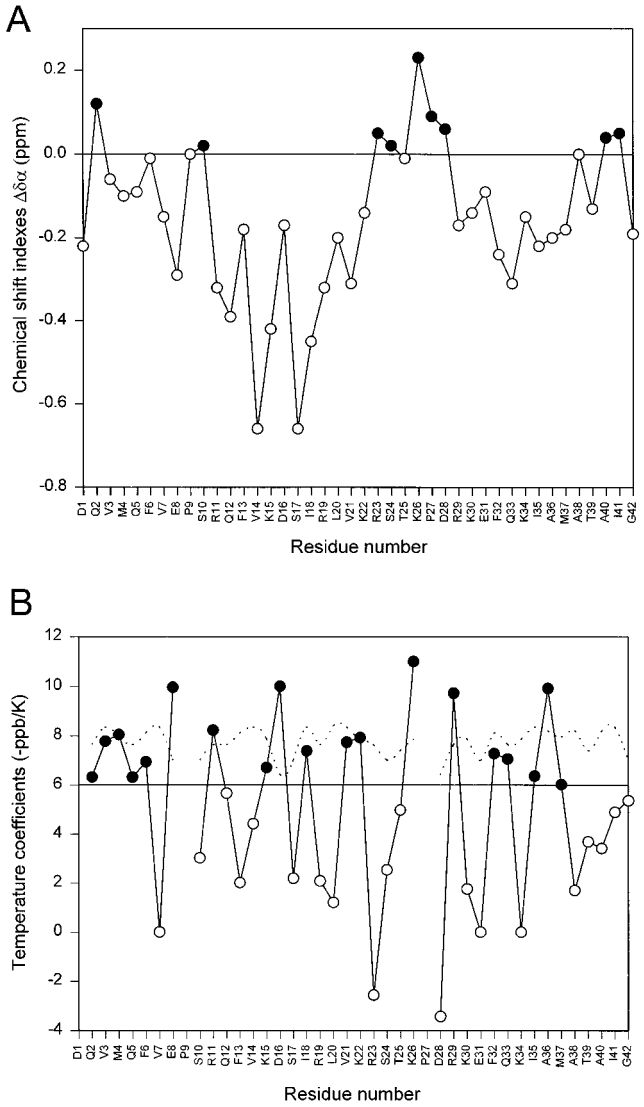

FIGURE 4: (A) α proton chemical shift indexes, $\Delta\delta\alpha = \delta\alpha_{obs} - \delta\alpha_{coil}$, for the peptide solubilized in the presence of DPC micelles at 38 °C and pH 5. Filled and hollow symbols respectively correspond to positive and negative $\Delta\delta\alpha$ values. (B) Temperature coefficients of the amide protons for the peptide solubilized in the presence of DPC micelles (solid line) and for random coil peptides (dashed line) (Merutka *et al.*, 1995). Filled and hollow symbols respectively correspond to temperature coefficients smaller and larger than −6 ppb/K.

both D28 and E31 amide signals (+3.5 and 0 ppb/K, respectively; Figure 4B). Second, we observed that the A-helix ends with two positively charged residues, K22-R23, known to have important capping ability at the helix C terminus (Bordo & Argos, 1994). Whereas the N-terminal capping box of the B-helix can be easily assessed from the NMR data, we have no direct evidence for the A-helix C-terminal capping. Indirect evidence may be found in the slightly positive $\Delta\delta\alpha$ value (Figure 4A), thus nonhelical, observed for R23, associated with the largely positive value (+3 ppb/K, Figure 4B) observed for its amide thermal coefficient, reflecting a strong hydrogen bonding. Third, the A-helix possesses a potential (i,i+3) salt bridge, D16−R19. This salt bridge formation is supported by the presence of an $\alpha\gamma$(16,19) NOE (Figure 3) and by the significant magnetic nonequivalence of the D16 $\beta\beta'$ and R19 $\gamma\gamma'$ signals (0.14 ppm for both methylene groups). Fourth, in the B-helix, residues E31−K34 may also form a salt bridge, competing with the capping structure. There is no experimental evidence for such a salt bridge apart from an ambiguous $\alpha\gamma$-(31,34) NOE (Figure 3). However, molecular modeling demonstrates that the D28−E31 capping box is not incompatible with an E31−K34 salt bridge and even with a reverse K26−E31 salt-bridge. In addition, the single R29 η-Q33 β NOE indicates an interaction between the R29 guanido group and the Q33 carboxamide group. Lastly, no tertiary structure which could have been revealed by interhelix NOE contacts, was observed.

Location of the α*−Loop−*α *Motif within the DPC Micelle.* Figure 4B shows the amide proton temperature coefficients plotted versus the residue number for the fragment in micelle. The values present a very large range of variation, extending from −11 to +4 ppb/K, together with a marked alternation. Amide proton thermal coefficients are related to hydrogen bond stability, that is to structural effects, as well as to water molecule accessibility. However, given the homogeneous secondary structure revealed by other NMR data, structural effects cannot account for such an amplitude and distribution of the thermal coefficients. On the other hand, most of the A-helix residues exhibiting a low amide thermal coefficient have their amide group mainly located in the apolar side of this amphipathic helix. Thus, the marked alternation of the thermal coefficients rather indicates that the peptide experiences two different environments at the same time. This result is clearly consistent with the A-helix lying at the membrane interface which is expected for a highly amphipathic helix exhibiting 10 apolar residues on one side and 8 charged plus 4 polar residues on the other side. For the B-helix residues, there is no correlation between the thermal coefficient values and the polarity of the residues as for the A-helix. This may result from a different average location of the B-helix in the membrane interface; for instance, the hydrophobic C-terminal part of the peptide, about five residues, might point toward the lipidic interior. In conclusion, the cytoplasmic domain of Sec61γ constitutes a well-defined α−loop−α motif with at least one helix lying at the membrane interface.

Comparison with Homologous Proteins. The sequence of a number of Sec61γ homologues from different organisms is available (Hartmann *et al.*, 1994; Murphy & Beckwith, 1994) (Figure 5). The N-terminal parts of the corresponding cytoplasmic domain of these homologous proteins are quite different in length and generally have unrelated sequences apart from their conserved amphipathic nature. The SecE of *Escherichia coli* represents a very special case since its N-terminal domain comprises two transmembrane segments. In contrast, there are several striking sequence conservations in the homologous segment approximately corresponding to the canine K22−F32 segment (Figure 5). The remarkable conservation concerns the A-helix C-terminal capping Lys/Arg residues and the N-capping residues of the B-helix, including the Pro residue. The conservation of a capping box motif, PDXXE or P(S/T)XX(E/Q), at the B-helix N terminus is impressive. There are two exceptions, *Bacillus subtilis* and *Bacillus licheniformis*, with the particular PKGKE sequence where the standard N cap residue D, S, or T is replaced by an ordinarily noncapping Lys residue but where the following, N cap + 1, residue is now a Gly. Such a possible capping sequence has not yet been described.

Finally, these elements of conservation markedly suggest that the P9−K34 α−loop−α motif constitutes the minimal

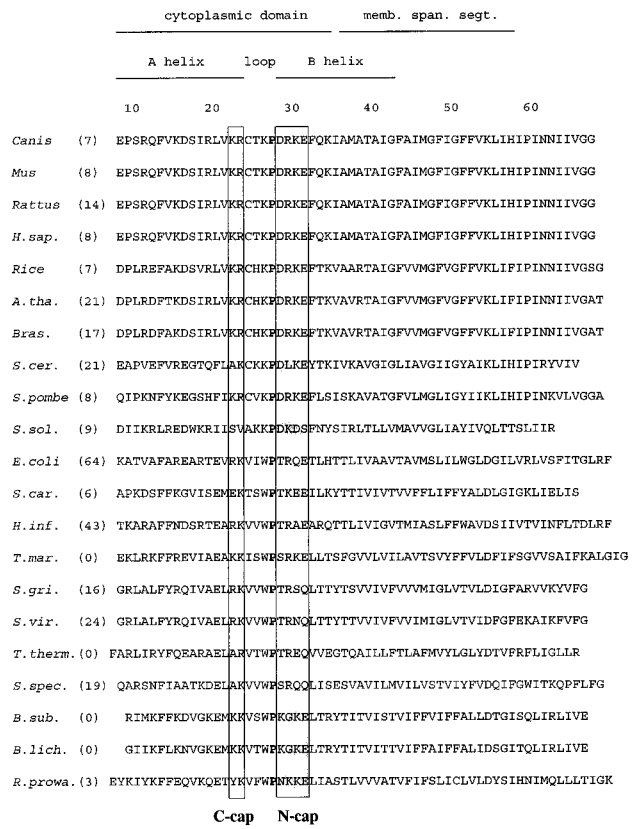

FIGURE 5: Alignment of the eukaryotic Sec61γ sequences with the bacterial SecEp sequences. Most of the sequences were obtained from Hartmann *et al.* (1994) and Murphy and Beckwith (1994). The numbers in parentheses correspond to the remaining N-terminal residues *not indicated* in the figure. The conserved proline is indicated in bold. The potential N-capping box and C-capping residues are framed. Residue numbering corresponds to the canine Sec61γ. Amino acid sequences from *Canis*, *Mus*, *Rattus*, *Homo sapiens* (*H.sap.*), *Rice*, *Arabidopsis thaliana* (*A.tha.*), *Brassica campestris* (*Bras.*), *Saccharomyces cerevisiae* (*S.cer.*), *Schizosaccharomyces pombe* (*S.pombe*), *Sufolobus solfataricus* (*S.sol.*), *Escherichia coli* (*E.coli*), *Staphylococcus carnosus* (*S.car.*), *Haemophilus influenzae* (*H.inf.*), *Thermogata maritima* (*T.mar.*), *Streptomyces griseus* (*S.gri.*), *Streptomyces virginiae* (*S.vir.*), *Thermus thermophilus* (*T.therm.*), *Synechocystis sp.* (*S.spec.*), *Bacillus subtilis* (*B.sub.*), *Bacillus licheniformis* (*B.lich.*), and *Rickettsia prowazekii* (*R. prowa.*).

structure for the cytoplasmic domain of the Sec61γ/SecE component of the translocation pore. Interestingly, the length of the canine Sec61γ P9−K34 segment corresponds, within very few residues, not only to the length of the smallest known SecE, namely that of *B. subtilis* , *B. licheniformis* and *Thermogata maritima*, but also to the shortest active fragment of the very much longer *E. coli* SecE described by Murphy and Beckwith (1994).

Modeling the Entire Sec61γ Protein. The signals of secondary structure which are encoded in the sequence of the Sec61γ family are rather strong and can be used to build a compact model of the entire protein. These signals are the two previously described capping structures and the end-of-helix signal constituted by the K54−H57 doublet after the stretch of 19 hydrophobic residues, I35−V53. The histidine residue is indeed a quite common residue found at the Ccap position in helices (Sali *et al.*, 1988; Dasgupta *et al.*, 1993) as it is also the case for the lysine residue at the C2 and C3 position (Ccap−2 and Ccap−3). Our *first assumption* to build the Sec61γ structure is thus the occurrence, at the end of the predicted transmembrane helix, of a C-terminal break at the H57 residue thus considered as the C-cap residue. Our *second assumption* is that the D28−H57 segment constitutes a single helix, roughly oriented parallel to the bilayer normal. The reason for this is the absence of helix-breaking signal other than the DXXE capping box already described. The only residue that could participate in a helix break, as an N-terminal capping residue, is T39. However, threonine residues are frequently found in transmembrane helices with no capping, i.e. helix-breaking property (see for instance the structure of the *viridis* reaction center; Deisenhofer *et al.*, 1989), and thus, in this context of transmembrane helix, the single T39 residue was not considered as a helix-breaking signal. The *last assumption* concerns the topology of the two helices. Interactions with the membrane surface impose on the markedly amphipathic A-helix a severe restriction on its axial rotational freedom. This restriction results in topological constraints on the disposition of the transmembrane B-helix with respect to the A-helix. If, in addition, the two helices are constrained to interact, then the available topologies reduce to two approximately mirror and *a priori* equivalent topologies, which roughly places the B-helix on either side of the A-helix.

Modeling the entire protein is now rather straightforward. The two helices were first positioned at a right angle in either main topologies and initially set to contact themselves in the region of their extremities in order to form a minimum compact structure. In a second step, the loop residues, R23−D28, and the C-terminal fragment, H54−G67, were annealed with the sole capping constraints relative to R23, D28−E31, and H54. The whole structures were then minimized as described in Materials and Methods. The two models were subsequently subjected to a 20 ps dynamics at 300 K *without any interhelix constraints*. Only one topology gave a stable structure, and the corresponding model is presented in Figure 6. The stability of this configuration can be explained by the two following features: (i) it allows the formation of a hydrophobic core involving L20, I35, and A38 and (ii) it allows the formation of an abundant hydrogen bond network between the two helices, namely D16−K34 and R19−E31. In the reverse topology, the loop is much more constrained and does not allow any stable contact between the two helices which are left floating around each other. Two criteria can be used to validate the main features of the model, namely the distribution of the hydrophilic residues with respect to the reference membrane interface and the distribution of the hydrophobic residues with respect to the membrane thickness. In Figure 6, the phospholipidic bilayer is represented by two phospholipid molecules (partially disordered POPC) delineating a biological membrane with the appropriate thickness, that is ∼38 Å between the two opposite glycerol C2 atoms (White, 1994). One can thus observe that the polar N-terminal segment D28−K34 of the B-helix, the hydrophilic loop, and the hydrophilic face of the A-helix can be located in the same region with respect to the reference membrane surface and, as a consequence, exactly occupy the *ca.* 8 Å thick phospholipidic interfacial region which comprises the glycerol and the polar head parts. The bare hydrophobic part, I35−V53, of the transmembrane helix (full B-helix) covers 19 residues, that is 27 Å between α-carbons. Considering that the effective hydrophobic part of the helix can be reasonably defined as extending from residues I35 to H57, one obtains a length of 33 Å. This pretty well fits the membrane hydrophobic core. It is worth noting that the

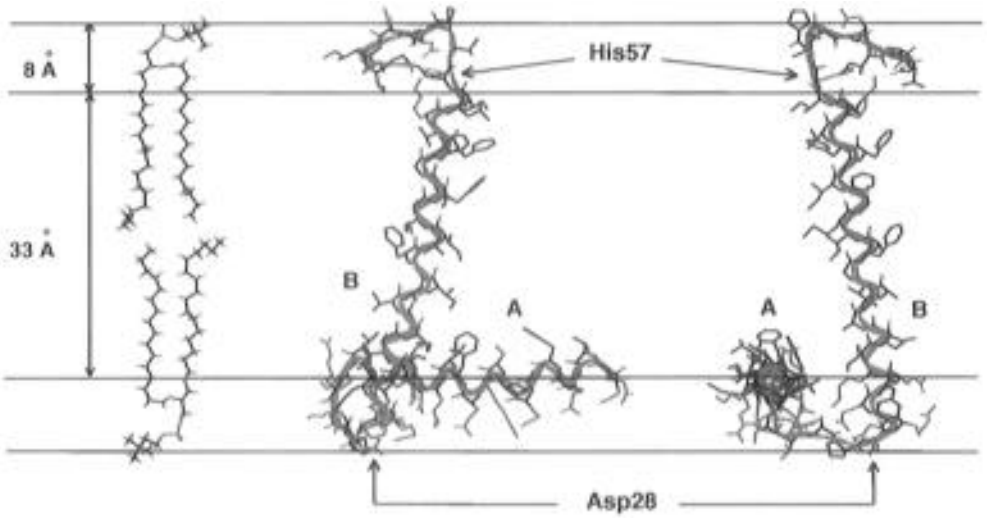

FIGURE 6: Two orthogonal views of the Sec61γ protein compact model within a reference membrane bilayer. The green ribbon corresponds to the fragment studied, and the orange ribbon corresponds to the remaining C-terminal part of the protein for which there is no experimental structural information available. Polar and apolar amino acid side chains are respectively colored orange and blue.

model shown in Figure 6 represents a reasonable structure with the maximum possible compactness. This means that we cannot rule out the protein having a loose structure that is simply composed of two rather independent helices, one parallel to the membrane normal and the other parallel to the membrane surface. This is what could be suggested by the absence of interhelix NOE contact in our 1−42 fragment micelle complex. However, the truncated transmembrane segment may not constitute a sufficient hydrophobic anchor in the context of a micelle environment to allow a correct fold of the fragment. More importantly, the C terminus of the truncated B-helix is, as for any helix, rather polar, and in spite of the hydrophobic nature of the last eight residues, the energy balance may not be markedly favorable to stable insertion into the micelle hydrophobic interior. As a consequence, the correct location of the truncated transmembrane segment may be impaired, and this may prevent further tertiary folding of the fragment.

Concluding Remarks. Our results give experimental support to the suggestion of Murphy and Beckwith (1994) relative to the existence of an amphipathic helix structure in the functionally important part of the C2 cytoplasmic domain linking the two last transmembrane helices of the *E. coli* SecE protein. Because of the strong homology between the SecE and Sec61γ proteins, our data establish that this part of the SecE C2 cytoplasmic domain rather corresponds to a helix−loop motif (A-helix−loop). This arrangement of the cytoplasmic domain, or better of the "interfacial domain", indeed makes the numerous basic side chains point into the cytoplasmic milieu and eventually available for interactions with cytosolic proteins. However, stress the very small length of interfacial domain of the smallest biologically active protein of the SecE/Sec61γ family (*Bacillus* sp., Figure 5) and the possibility that these proteins might only possess a loose structure. This raises the question of which is the actual active part of the protein. Our model may suggest the transmembrane segment, and more likely the loop region, as being in fact the active part of this small membrane protein. The consideration of the role of the positively charged A-helix in the interaction with specific phospholipids also remains.

SUPPORTING INFORMATION AVAILABLE

^{1}H chemical shifts for the peptide solubilized in aqueous solution at −1 °C and pH 5 and ^{1}H chemical shifts for the peptide solubilized in the presence of DPC micelles at 38 °C and pH 5 (2 pages). Ordering information is given on any current masthead page.

REFERENCES

Alexandrescu, A. T., Evans, P. A., Pitkeathly, M., Baum, J., & Dobson, C. M. (1993) *Biochemistry 32*, 1707−1718.
Bordo, D., & Argos, P. (1994) *J. Mol. Biol. 243*, 504−519.
Broadhurst, R. W., Dobson, C. M., Hore, P. J., Radford, S. E., & Rees, M. L. (1991) *Biochemistry 30*, 405−412.
Cordier-Ochsenbein, F., Guérois, R., Baleux, F., Huynh-Dinh, T., Chafotte, A., Neumann, J. M., & Sanson, A. (1996) *Biochemistry 35*,10347−10357.
Dasgupta, S., & Bell, J. A. (1993) *Int. J. Pept. Protein Res. 41*, 499−511.
Deisenhofer, J., & Michel, H. (1989) *Science 245*, 1463.
Deshaies, R. J., & Schekman, R. (1987) *J. Cell Biol. 105*, 633−645.
Esnault, Y., Blondel, M. O., Deshaies, R. J., Schekman, R., & Képès, F. (1993) *EMBO J. 12*, 4083−4093.
Esnault, Y., Feldheim, D., Blondel, M. O., Schekman, R., & Képès, F. (1994) *J. Biol. Chem. 269*, 27478−27485.
Evans, P. A., Topping, K. D., Woolfsson, D. N., & Dobson, C. M. (1991) *Proteins: Struct., Funct., Genet. 9*, 248−266.
Garvey, E. P., Swank, J., & Matthews, C. R. (1989) *Proteins: Struct., Funct., Genet. 6*, 259−266.
Görlich, D., & Rapoport, T. A. (1993) *Cell 75*, 615−630.
Harper, E. T., & Rose, G. D. (1993) *Biochemistry 32*, 7605−7609.
Hartmann, E., Sommer, T., Prehn, S., Görlich, D., Jentsch, S., & Rapoport, T. A. (1994) *Nature 367*, 654−657.
Jiménez, M. A., Muñoz, V., Rico, M., & Serrano, L. (1994) *J. Mol. Biol. 242*, 487−496.
Kay, E. L., Torchia, D. A., & Bax, A. (1989) *Biochemistry 28*, 8972−8979.
Lauterwein, J., Bösch, C., Brown, L. R., & Wüthrich, K. (1979) *Biochim. Biophys. Acta 556*, 244−264.
Lipari, G., & Szabo, A. (1982) *J. Am. Chem. Soc. 104*, 4546−4559.
Lumb, K. J., & Kim, P. S. (1994) *J. Mol. Biol. 236*, 412−420.
Lyu, P. C., Wemmer, D. E., Zhou, H. X., Pinker, R. J., & Kallenbach, N. R. (1993) *Biochemistry 32*, 412−425.
Macquaire, F., Baleux, F., Huynh-Dinh, T., Rouge, D., Neumann, J. M., & Sanson, A. (1993) *Biochemistry 32*, 7244−7254.
Merrifield, R. B. (1963) *J. Am. Chem. Soc. 85*, 2149−2154.

Merutka, G., Dyson, H. J., & Wright, P. E. (1995) *J. Biomol. NMR 5*, 14−24.
Muñoz, V., & Serrano, L. (1995) *J. Mol. Biol. 245*, 275−296.
Muñoz, V., Blanco, F. J., & Serrano, L. (1995) *Nat. Struct. Biol. 2*, 380−386.
Murphy, C. K., & Beckwith, J. (1994) *Proc. Natl. Acad. Sci. U.S.A. 91*, 2557−2561.
Neri, D., Billeter, M., Wider, G., & Wüthrich, K. (1992) *Science 257*, 1559−1563.
Panzner, S., Dreier, L., Hartmann, E., Kostka, S., & Rapoport, T. A. (1995) *Cell 81*, 561−570.
Plateau, P., & Guéron, M. (1982) *J. Am. Chem. Soc. 104*, 7310−7311.
Sali, D., Bycroft, M., & Fersht, A. R. (1988) *Nature 335*, 740−743.
Seale, J. W., Srinivasan, R., & Rose, G. D. (1994) *Protein Sci. 3*, 1741−1745.
Smith, L. J., Alexandrescu, A. T., Pitkeathly, M., & Dobson, C. M. (1994) *Structure 2*, 703−712.
Stirling, C. J., Rothblatt, J., Hosobuchi, M., Deshaies, R. J., & Schekman, R. (1992) *Mol. Biol. Cell 3*, 129−142.
Tam, J. P., & Heath, W. F. (1983) *J. Am. Chem. Soc. 105*, 6442−6447.
White, S. H. (1994) *Membrane Protein Structure*, Oxford University Press, New York.
Wishart, D. S., Sykes, B. D., & Richards, F. M. (1992) *Biochemistry 31*, 1647−1651.

BI961710D